Article

Photochemistry of Artificial Photosynthetic Reaction Centers in Liquid Crystals Probed by Multifrequency EPR (9.5 and 95 GHz)

Marilena Di Valentin, Arianna Bisol, Giancarlo Agostini, Michael Fuhs, Paul A. Liddell, Ana L. Moore, Thomas A. Moore, Devens Gust, and Donatella Carbonera

J. Am. Chem. Soc., **2004**, 126 (51), 17074-17086• DOI: 10.1021/ja046067u • Publication Date (Web): 02 December 2004

More About This Article

Additional resources and features associated with this article are available within the HTML version:

- Supporting Information
- Links to the 1 articles that cite this article, as of the time of this article download
- Access to high resolution figures
- Links to articles and content related to this article
- Copyright permission to reproduce figures and/or text from this article

View the Full Text HTML

J|A|C|S
ARTICLES
Published on Web 12/02/2004

Photochemistry of Artificial Photosynthetic Reaction Centers in Liquid Crystals Probed by Multifrequency EPR (9.5 and 95 GHz)

Marilena Di Valentin,*,† Arianna Bisol,† Giancarlo Agostini,‡ Michael Fuhs,† Paul A. Liddell,§ Ana L. Moore,§ Thomas A. Moore,§ Devens Gust,§ and Donatella Carbonera†

Contribution from the Università di Padova, Dipartimento di Scienze Chimiche, via Marzolo 1, I-35131 Padova, Italy; CNR-Istituto di Chimica Biomolecolare, Sezione di Padova, via Marzolo 1, I-35131 Padova, Italy; and Arizona State University, Department of Chemistry and Biochemistry, Center for the Study of Early Events in Photosynthesis, 85287-1604 Tempe, Arizona

Received July 2, 2004; E-mail: m.divalentin@chfi.unipd.it

Abstract: Photoinduced charge separation and recombination in a carotenoid−porphyrin−fullerene triad C−P−C_{60}[1] have been followed by multifrequency time-resolved electron paramagnetic resonance (TREPR) at intermediate magnetic field and microwave frequency (X-band) and high field and frequency (W-band). The electron-transfer process has been characterized in the different phases of two uniaxial liquid crystals (E-7 and ZLI-1167). The triad undergoes photoinduced electron transfer, with the generation of a long-lived charge-separated state, and charge recombination to the triplet state, localized in the carotene moiety, mimicking different aspects of the photosynthetic electron-transfer process. Both the photoinduced spin-correlated radical pair and the spin-polarized recombination triplet are observed starting from the crystalline up to the isotropic phase of the liquid crystals. The W-band TREPR radical pair spectrum has allowed unambiguous assignment of the spin-correlated radical pair spectrum to the charge-separated state $C^{\bullet+}$−P−$C_{60}^{\bullet-}$. The magnetic interaction parameters have been evaluated by simulation of the spin-polarized radical pair spectrum and the spin-selective recombination rates have been derived from the time dependence of the spectrum. The weak exchange interaction parameter ($J = +0.5 \pm 0.2$ G) provides a direct measure of the dominant electronic coupling matrix element V between the $C^{\bullet+}$−P−$C_{60}^{\bullet-}$ radical pair state and the recombination triplet state ^{3}C−P−C_{60}. The kinetic parameters have been analyzed in terms of the effect of the liquid crystal medium on the electron-transfer process. Effects of orientation of the molecular triad in the liquid crystal are evidenced by simulations of the carotenoid triplet state EPR spectra at different orientations of the external magnetic field with respect to the director of the mesophase. The order parameter ($S = 0.5 \pm 0.05$) has been evaluated.

Introduction

Ensembles of covalently linked electron donor and acceptor moieties have long been investigated as models for the stepwise photoinduced electron-transfer process observed in the reaction centers of photosynthetic organisms.[2−7] Fullerene derivatives have been found to be excellent electron acceptors and have been incorporated in many molecular dyads and triads that act as artificial reaction centers.[8−11] They have small internal and solvent reorganization energies and low sensitivity to solvent stabilization of their anions.[1,12−15] These features all together lead to rapid forward photoinduced electron transfer (ET) and slow charge recombination.

Among these molecular systems, three carotenoid (C), porphyrin (P), and fullerene (C_{60}) molecular triads, differing one from the other due to small structural changes, have been prepared and extensively investigated by both optical and

† Università di Padova.
‡ CNR-Istituto di Chimica Biomolecolare.
§ Arizona State University.

(1) Kuciauskas, D.; Liddell, P. A.; Lin, S.; Stone, S. G.; Moore, A. L.; Moore, T. A.; Gust, D. *J. Phys. Chem. B* **2000**, *104*, 4307−4321.
(2) Gust, D.; Moore, T. A. *Top. Curr. Chem.* **1991**, *159*, 103−151.
(3) Wasielewski, M. R. *Chem. Rev.* **1992**, *92*, 435−461.
(4) Kurreck, H.; Huber, M. *Angew. Chem., Int. Ed. Engl.* **1995**, *34*, 849−866.
(5) Gust, D.; Moore, T. A.; Moore, A. L. *Pure Appl. Chem.* **1998**, *70*, 2189−2200.
(6) Gust, D.; Moore, T. A. In *The Porphyrin Handbook*; Kadish, K. M., Smith, K. M., Guilard, R., Eds.; Academic Press: New York, 2000; Vol. 8, pp 153−190.
(7) Moore, T. A.; Moore, A. L.; Gust, D. *Philos. Trans. R. Soc. London, Ser. B* **2002**, *357*, 1481−1498.
(8) Imahori, H.; Sakata, Y. *Adv. Mater.* **1997**, *9*, 537−546.
(9) Guldi, D. M. *Chem. Soc. Rev.* **2002**, *31*, 22−36.
(10) Meijer, M. D.; van Klink, G. P. M.; van Koten, G. *Coord. Chem. Rev.* **2002**, *230*, 141−163.
(11) Guldi, D. M. *Pure Appl. Chem.* **2003**, *75*, 1069−1075.
(12) Larsson, S.; Klimkāns, A.; Rodriguez-Monge, L.; Duškesas, G. *THEOCHEM* **1998**, *425*, 155−159.
(13) Guldi, D. M. *Chem. Commun.* **2000**, 321−327.
(14) Imahori, H.; Yamada, H.; Guldi, D. M.; Endo, Y.; Shimomura, A.; Kundu, S.; Yamada, K.; Okada, T.; Sakata, Y.; Fukuzumi, S. *Angew. Chem., Int. Ed.* **2002**, *41*, 2344−2347.
(15) Guldi, D. M.; Luo, C.; Kotov, N. A.; Da Ros, T.; Bosi, S.; Prato, M. *J. Phys. Chem. B* **2003**, *107*, 7293−7298.

10.1021/ja046067u CCC: $27.50

Scheme 1. Structure of Triad **1**

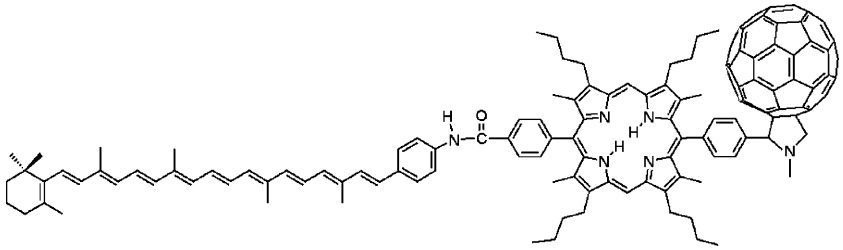

magnetic time-resolved spectroscopies.[1,16−21] They all feature several key properties of the reaction center primary photochemistry, which have been successfully mimicked by a few artificial model systems. These include a high yield of charge separation, photoinduced ET in the glass at low temperature, charge recombination to a triplet state, and photoprotection from singlet oxygen damage by an activated triplet energy transfer relay mechanism.[19] The small structural differences between the C−P−C_{60} molecular triads have been used to investigate the effects of driving force and electronic coupling on yields and rate constants.[20]

A complete study of the photophysical behavior of triad **1** (see Scheme 1) as a function of temperature and solvent has been performed.[1]

In a variety of polar solvents, excitation of the porphyrin moiety yields the first excited singlet state C−^{1}P−C_{60}, which undergoes photoinduced electron transfer to give C−$P^{\bullet+}$−$C_{60}^{\bullet-}$. Electron transfer from the carotenoid moiety competes with charge recombination, leading to the formation of a final $C^{\bullet+}$−P−$C_{60}^{\bullet-}$ charge-separated state. This state is generated with quantum yields up to 0.88 and has a lifetime of up to 1 μs, depending upon the conditions. In most solvents, charge recombination of the secondary charge-separated state yields the carotenoid triplet state ^{3}C−P−C_{60}, rather than the singlet ground state. Triplet recombination of $C^{\bullet+}$−P−$C_{60}^{\bullet-}$ is favored because the energy of the carotenoid triplet state is significantly below that of the secondary charge-separated state.[22] The photochemistry of triad **1** is illustrated in Figure 1.

Triplet recombination, which is a peculiar property of all the C−P−C_{60} molecular triads and is found only in a few model systems,[23,24] reproduces the recombination process between the special pair primary donor and an acceptor occurring in natural photosynthetic reaction centers after prereduction or removal of secondary electron acceptors.[25]

The mimicry of the photosynthetic process has been extended even further by inserting vectorially the artificial reaction centers into lipid bilayers to exploit the photoinduced charge separated states for driving the transport of ions across such membranes.[26,27]

To mimic the anisotropic surroundings found in membranes, artificial molecular systems have also been embedded in liquid crystal (LC) solvents.[4,28,29] LCs are convenient media for time-resolved electron spin resonance (TREPR) studies of photoinduced ET.[28,29] The ET process may be brought in the solvent-controlled adiabatic limit due to the restricted mobility of the molecules in the presence of the nematic potential, slowing down in this way the ET rates in the TREPR time scale. The radical pair and triplet paramagnetic species can be detected in the solid and in the fluid nematic phases over a wide temperature range, allowing fine-tuning of the reorganization energy of the system. The anisotropy imposed by the nematic potential introduces orientational effects on the spectra, which can be used to derive the magnetic interaction parameters.

A preliminary TREPR investigation of triad **1** in the uniaxial liquid crystal E-7 has been reported.[21] Two-step charge separation and charge recombination to the triplet state, localized in the carotene moiety, occur in all the different phases of the liquid crystal. The high degree of ordering in the LC achieved by molecular triad **1** and the possibility of following the radical pair recombination kinetics over a wide temperature range in the LC medium have stimulated a TREPR study of triad **1** in the anisotropic solvent and an extension of the investigation to the ZLI-1167 LC, which features complementary properties to E-7, with the orientation of the mesophase director spanning the plane perpendicular to the static magnetic field instead of lying parallel to it.[30−32]

This study combines time-resolved X-band (9.5 GHz) and W-band (95 GHz) EPR experiments on the molecular triad in the different phases of the E-7 and ZLI-1167. Improved spectral and dynamic resolution at higher Zeeman fields allowed unambiguous identification of the partners of the spin-correlated radical pair, derivation of the magnetic interaction parameters, the dipolar and exchange interaction between the two electron paramagnetic spins, and determination of the genesis and recombination kinetics of the $C^{\bullet+}$−P−$C_{60}^{\bullet-}$ charge-separated radical pair.

(16) Liddell, P. A.; Kuciauskas, D.; Sumida, J. P.; Nash, B.; Nguyen, D.; Moore, A. L.; Moore, T. A.; Gust, D. *J. Am. Chem. Soc.* **1997**, *119*, 1400−1405.
(17) Carbonera, D.; Di Valentin, M.; Corvaja, C.; Agostini, G.; Giacometti, G.; Liddell, P. A.; Kuciauskas, D.; Moore, A. L.; Moore, T. A.; Gust, D. *J. Am. Chem. Soc.* **1998**, *120*, 4398−4405.
(18) Kuciauskas, D.; Liddell, P. A.; Moore, A. L.; Moore, T. A.; Gust, D. *J. Am. Chem. Soc.* **1998**, *120*, 10880−10886.
(19) Gust, D.; Moore, T. A.; Moore, A. L.; Kuciauskas, D.; Liddell, P. A.; Halbert, B. D. *J. Photochem. Photobiol. B* **1998**, *43*, 209−216.
(20) Bahr, J. L.; Kuciauskas, D.; Liddell, P. A.; Moore, A. L.; Moore, T. A.; Gust, D. *Photochem. Photobiol.* **2000**, *72*, 598−611.
(21) Di Valentin, M.; Bisol, A.; Giacometti, G.; Carbonera, D.; Agostini, G.; Liddell, P. A.; Moore, A. L.; Moore, T. A.; Gust, D. *Mol. Cryst. Liq. Cryst.* **2003**, *394*, 19−30.
(22) Lewis, J. E.; Moore, T. A.; Benin, D.; Gust, D.; Nicodem, D.; Nonell, S. *Photochem. Photobiol*. **1994**, *59S*, 35.
(23) Hasharoni, K.; Levanon, H.; Greenfield, S. R.; Gosztola, D. J.; Svec, W. A.; Wasielewski, M. R. *J. Am. Chem. Soc.* **1996**, *118*, 10228−10235.
(24) Wiederrecht, G. P.; Svec, W. A.; Wasielewski, M. R.; Galili, T.; Levanon, H. *J. Am. Chem. Soc*. **2000**, *122*, 9715−9722.
(25) McGann, W. J.; Frank, H. A. *Chem. Phys. Lett.* **1985**, *121*, 253−261.
(26) Steinberg-Yfrach, G.; Rigaud, J.-L.; Durantini, E. N.; Moore, A. L.; Gust, D.; Moore, T. A. *Nature* **1998**, *392*, 479−482.
(27) Bennett, I. M.; Vanegas Farfano, H. M.; Bogani, F.; Primak, A.; Liddell, P. A.; Otero, L.; Sereno, L.; Silber, J. J.; Moore, A. L.; Moore, T. A.; Gust, D. *Nature* **2002**, *420*, 398−401.
(28) Levanon, H.; Hasharoni, K. *Prog. React. Kinet*. **1995**, *20*, 309−346.
(29) Levanon, H.; Möbius, K. *Annu. Rev. Biophys. Biomol. Struct*. **1997**, *26*, 495−540.
(30) Hasharoni, K.; Levanon, H.; von Gersdorff, J.; Kurreck, H.; Möbius, K. *J. Chem. Phys.* **1993**, *98*, 2916−2926.
(31) Levanon, H.; Galili, T.; Regev, A.; Wiederrecht, G. P.; Svec, W. A.; Wasielewski, M. R. *J. Am. Chem. Soc*. **1998**, *120*, 6366−6373.
(32) Asano-Someda, M.; Levanon, H.; Sessler, J. L.; Wang, R. *Mol. Phys.* **1998**, *95*, 935−942.

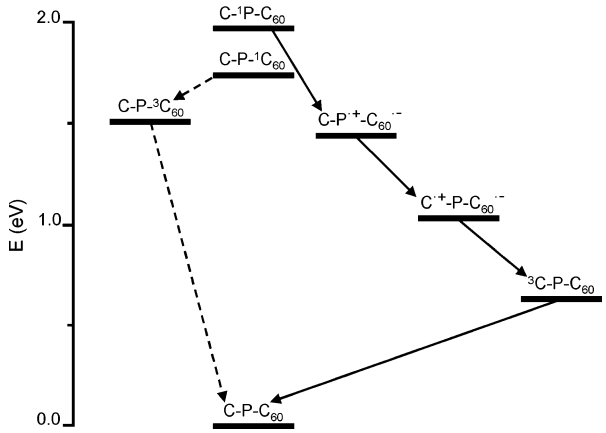

Figure 1. Relevant high energy states and interconversion pathways for triad **1** following excitation. The energies of the various states have been estimated from spectroscopic and cyclic voltammetric data obtained in polar solvents.[1]

The magnitude of the exchange interaction between the unpaired electrons gives information on the electronic structure of the radical pair and on the possible role of the molecular bridge in mediating the interaction between the two electronic spins. The exchange parameter provides a direct measure of the electronic coupling element V between the radical pair state and the electronic states that are energetically close.[33−36] In this work, the exchange interaction J between the carotene radical cation and the fullerene radical anion has been used to estimate the dominant electronic coupling matrix element V that connects the $C^{\bullet+}-P-C_{60}^{\bullet-}$ radical pair state to the recombination triplet localized on the carotene moiety $^3C-P-C_{60}$ and to discuss it in relation to the ET rate constant and the reorganization energy of this fullerene-based molecular system.[1,9] Moreover, the value of the J parameter obtained from simulations confirms the previous hypothesis of an exchange interaction between the carotene donor and the fullerene electron acceptor mediated by the porphyrin bridge.[17,21]

The lack of any reduction in recombination rate induced by the nematic potential of the LC[37] has also been discussed and related to the electronic coupling element V of the $C^{\bullet+}-P-C_{60}^{\bullet-}$ radical pair state, to confirm the estimation of the J parameter derived from simulations.

Experimental Section

X-band time-resolved EPR spectra were obtained using a pulsed laser light guided into an X-band EPR spectrometer (Bruker ER 200D) equipped with a low-Q TE_{001} cavity (9.4 GHz) and a nitrogen flow system. The microwave power used for the TREPR experiments was about 20 mW at the cavity. The time resolution of the TREPR spectrometer is about 200 ns. In initial experiments laser excitation at 580 nm (10 mJ per pulse and repetition rate 20 Hz) was provided by an excimer laser pumping a Rhodamin 6G dye laser. Thereafter laser excitation at 532 nm (10 mJ per pulse and repetition rate 10 Hz) was provided by the second harmonic of a Nd:YAG laser. Excitation at both wavelengths yields mostly $C-^1P-C_{60}$. No effect on the EPR spectra was produced by changing the excitation wavelength. The TREPR experiments were performed in direct detection mode, without field modulation. The EPR signals were taken from the microwave preamplifier (ER047-PH Bruker, bandwidth 20 Hz-6.5 MHz) and sampled with a LeCroy 9361 oscilloscope (3 ns per point). To eliminate the laser background signal, transients were accumulated at off-resonance field conditions and subtracted from those on resonance. The spectra at different times after the laser pulse were reconstructed from kinetic traces for each field position.

W-band TREPR spectra were measured in direct detection mode using a laboratory-built 95 GHz high field EPR spectrometer, which has been described in detail elsewhere.[38] The time resolution is about 10 ns. Laser excitation at 532 nm (10 mJ per pulse and repetition rate 10 Hz) was provided by the second harmonic of a Nd:YAG laser. The microwave power that was used for the TREPR experiments was about 0.25 mW at the cylindrical cavity. For each magnetic field position, the signal was averaged over the indicated integration window after the laser pulse and the average of an equivalent integration window before the laser pulse was subtracted.

The synthesis of triad **1** has been reported.[1] The TREPR experiments were performed on the molecular triads embedded and oriented in the liquid crystals E-7 and ZLI-1167 (Merck Ltd.). E-7 is characterized by a positive diamagnetic susceptibility $\Delta\chi$ and a longitudinal dielectric constant $\epsilon_{||} = 19.6$, while ZLI-1167 has a negative $\Delta\chi$ and $\epsilon_{||} = 7.5$. The two LCs are characterized by the following phase transition temperatures:

E-7: crystalline ←210 K→ soft glass ←263 K→ nematic ←333 K→ isotropic.

ZLI-1167: crystalline ←287 K→ smectic ←305 K→ nematic ←356 K→ isotropic.

For the X-band experiments, the samples ($\sim 5 \times 10^{-4}$ M) were prepared by dissolving triad **1** in toluene solution, evaporating the solvent and then introducing E-7. They were afterward deaerated by several freeze−thaw cycles and sealed under vacuum in thin-walled quartz tubes of a 4 mm outer diameter. For the W-band experiments 0.5 mm quartz capillaries were used. Samples were flushed with nitrogen inside the capillary for at least 20 min at the temperature at which the isotropic phase of the LC is reached. The sample concentration was about 5×10^{-4} M.

For the X-band experiments, the alignment of the samples was carried out in the nematic phase under an external magnetic field of 6000 G for 10 min followed, if necessary, by fast cooling to the required temperature in the crystalline phase, under the same magnetic field conditions.[30] In the fluid nematic phase of E-7, the director **L** is aligned parallel to the external magnetic field **B**. In the crystalline phase of E-7 different sample orientations, in terms of **L** with respect to the magnetic field, were investigated; **L** || **B**, the parallel configuration, is the default orientation caused by the alignment, and the other orientations were reached by turning the sample, mounted on a goniometer, in the cavity about an axis perpendicular to the external magnetic field. For the W-band experiments, the sample alignment was achieved at the high magnetic field conditions of the experiments.

The optimized ground-state geometry of the $C-P-C_{60}$ triad was calculated using ChemBats3D (MM2). Simulations of the partially ordered triplet spectra were performed using a home-written FORTRAN program, while the time development of the spin-correlated radical pair spectra in partially ordered media were calculated using home-written programs in MATLAB.

Results

TREPR in the Liquid Crystal E-7. Figure 2 shows the X-band spin-polarized EPR spectra of triad **1** at 350 ns after the laser pulse in the crystalline phase of E-7 at 150 K, in the

(33) Anderson, P. W. *Phys. Rev.* **1959**, *115*, 2−13.
(34) Volk, M.; Häberle, T.; Feick, R.; Ogrodnik, A.; Michel-Beyerle, M.-E. *J. Phys. Chem.* **1993**, *97*, 9831−9836.
(35) Calvo, R.; Abresch, E. C.; Bittl, R.; Feher, G.; Hofbauer, W.; Isaacson, R. A.; Lubitz, W.; Okamura, M. Y.; Paddock, M. L. *J. Am. Chem. Soc.* **2000**, *122*, 7327−7341.
(36) Weiss, E. A.; Ratner, M. A.; Wasielewski, M. R. *J. Phys. Chem. A* **2003**, *107*, 3639−3647.
(37) Hasharoni, K.; Levanon, H. *J. Phys. Chem.* **1995**, *99*, 4875−4878.
(38) Prisner, T. F.; Rohrer, M.; Moebius, K. *Appl. Magn. Reson.* **1994**, *7*, 167−183.

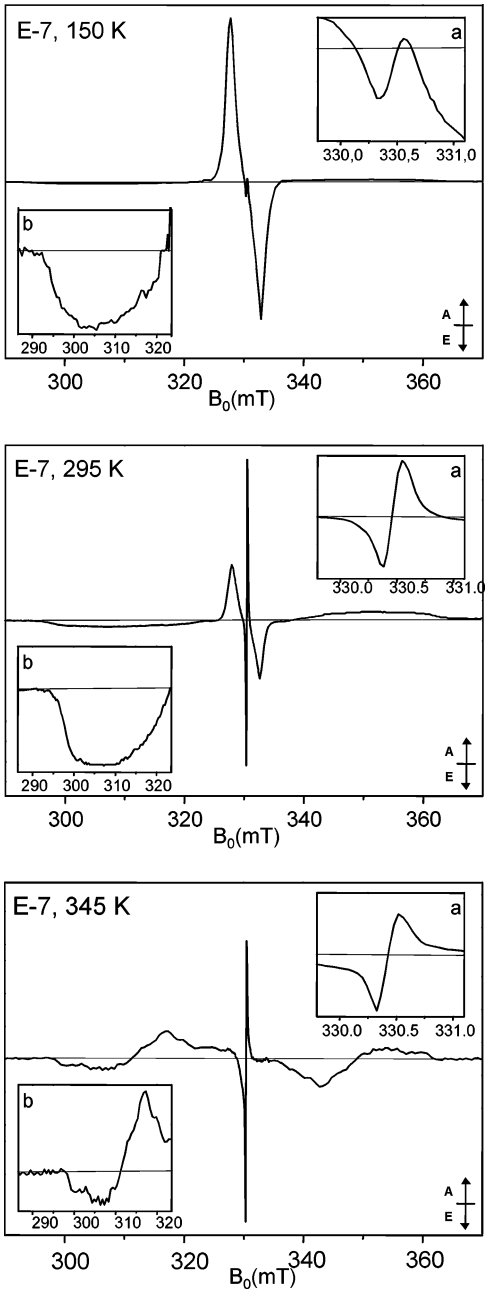

Figure 2. X-band TREPR spectra of the C−P−C_{60} triad in the crystalline (T = 150 K), in the nematic (T = 295 K), and in the isotropic (T = 345 K) phases of the LC E-7 (L || B), at 350 ns after the laser pulse. The insets display (a) the expanded TREPR spectra in the radical pair region and (b) the expanded TREPR spectra in the carotenoid triplet low-field region. A = absorption, E = emission.

nematic phase at 295 K and in the isotropic phase at 345 K. The TREPR spectrum in the nematic phase of E-7 was already reported, and all the paramagnetic species present in the spectra have been assigned in the preliminary work.[21] The narrow signal at the center of the spectrum (insets a in Figure 2) can be attributed to the $C^{\bullet+}-P-C_{60}^{\bullet-}$ radical pair state.

The broad contribution spanning ~50 mT (insets b in Figure 2) comes from the carotenoid triplet ($^3C-P-C_{60}$), and the narrower triplet contribution spanning ~20 mT is due to the fullerene triplet ($C-P-^3C_{60}$). The assignment of the triplet spectra is based on the zero-field-splitting (ZFS) parameters derived from EPR experiments on model compounds.[39−41] In the crystalline and nematic phases, the carotenoid and fullerene triplet spectra show a high degree of order in the LC medium when compared to the corresponding powder spectra in 2-MeTHF glass.[17,21] In the isotropic phase the carotenoid triplet is still detectable and a random distribution of orientations is achieved, accompanied by partial averaging of the ZFS parameters.

While in the crystalline phase of E-7 the main contribution to the spectrum is the partially oriented fullerene triplet; in the nematic and isotropic phases the narrow radical pair signal becomes the major contribution. Charge separation also occurs in the glass phase of the LC, where the motions of the solvent molecules are restricted, as found for the isotropic glass of 2-MeTHF. Charge separation is achieved in high quantum yields in the overall range of the nematic phase (up to 320 K). Even in the isotropic phase (up to 360 K) a spin-polarized radical pair signal has been observed and no thermal spin equilibrium is reached. The radical pair signal shows only the doublet contribution coming from the narrow fullerene radical anion. The observation of only one of the two derivative-like EPR signals in the radical pair spectrum can be ascribed to hyperfine broadening of the e/a line corresponding to the carotenoid radical. This line is further obscured by the superposition with the fullerene triplet state signal.

The decay of the narrow radical pair signal is correlated to the rise of the carotenoid triplet signal at all the ZFS canonical orientations, proving that the carotenoid triplet is formed by charge recombination in all the different phases of the LC. The correlation in the nematic phase of E-7 was already reported.[21] Further evidence of triplet recombination comes from the spin polarization pattern of the carotenoid triplet spectrum. While, in the 2-MeTHF glass, the powder triplet spectrum clearly shows the eaaeea pattern produced by charge recombination of a singlet-born radical pair,[17,21] the partially ordered triplet spectrum obtained in the crystalline and nematic phases of the LC solvent shows only contributions in emission at low field and in absorption at high field due to some particular molecular orientations which are parallel to the director of the mesophase (the low-magnetic-field semispectra are shown in insets b of Figure 2). To prove that, also in the LC, the overall polarization pattern is in agreement with that of a recombination triplet with a singlet precursor, the EPR spectra in the carotenoid triplet spectral range have been recorded at different orientations of the ordering director (**L**) relative to the external magnetic field (**B**). The experimental semispectra of the carotenoid triplet state, taken 900 ns after the laser pulse (corresponding to the maximum intensity of carotenoid triplet signal) in the ordered glass of the LC solvent, are reported in panel a of Figure 3.

The spectra differ in terms of the orientation of the ordering director with the external magnetic field. The different orientations have been achieved by rotation of the sample in the cavity about an axis perpendicular to the external magnetic field, in the crystalline phase of E-7. The high degree of ordering of the LC sample is evident in the strong orientation dependence of the triplet spectra.

Simulations of the carotenoid triplet spectra in the partially ordered glass, at the different orientations of **L** with respect to

(39) Carbonera, D.; Di Valentin, M.; Agostini, G.; Giacometti, G.; Liddell, P. A.; Gust, D.; Moore, A. L.; Moore, T. A. *Appl. Magn. Reson.* **1997**, *13*, 487−504.
(40) Pasimeni, L.; Segre, U.; Ruzzi, M.; Maggini, M.; Prato, M.; Kordatos, K. *J. Phys. Chem. B* **1999**, *103*, 11275−11281.
(41) Ceola, S.; Corvaja, C.; Franco, L. *Mol. Cryst. Liq. Cryst.* **2003**, *394*, 31−43.

B, have been performed to derive the spin polarization pattern. They are based on a theoretical approach that has been described in detail.[42] For an axially symmetric molecule, as approximated by triad **1**, which is characterized by a long molecular axis, the mean field orienting potential can be written as a function of only one angle (ψ), which describes the orientation of the molecular symmetry axis of the guest molecules with respect to the director of the mesophase **L**:

$$U(\psi) = \frac{\lambda k_B T(3\cos^2\psi - 1)}{2} \quad (1)$$

where the dimensionless parameter λ measures the strength of the orienting potential.

The alignment of the guest molecules is characterized by the order parameter, defined as the orientation average:

$$S = \left\langle \frac{(3\cos^2\psi - 1)}{2} \right\rangle \quad (2)$$

In addition, triplet spectra simulations depend also on the ZFS parameters, D and E, and on the relative populations of the triplet sublevels.

In Figure 3 the experimental triplet semispectra (panel a) have been compared with the corresponding calculated spectra (panel b). The outcome of the analysis, in terms of relative populations of the triplet sublevels, shows that the polarization pattern in the partially ordered environment is characteristic of a triplet populated by recombination of a singlet radical pair, exclusively in the T_0 high-field spin level. The ZFS parameters are in good agreement with those derived for the carotenoid triplet in carotenoporphyrin dyads in 2-MeTHF ($|D| = 0.0346$ cm^{-1}, $|E| = 0.0035$ cm^{-1}),[39] confirming therefore the assignment of the broad triplet signal to the carotenoid triplet. The simulations verify that a high degree of order is induced by the orienting potential of the LC on the guest triad molecules ($S = 0.5 \pm 0.05$). Furthermore, by combining the information on the location of the carotenoid triplet ZFS axes relative to the molecular frame with low-energy conformation data, the orientation of the molecular triad with respect to the alignment axis can be inferred. The orientations of the principal axes of the ZFS tensor relative to the molecular frame are known. They have been derived by Frick et al. in a single-crystal EPR work on the β-carotene triplet state.[43] The z axis, which is associated with the largest value Z of the ZFS tensor, is the long molecular chain axis; the x axis is the normal to the in-chain plane; and the y axis, associated with the smallest ZFS component, is the normal to the out-of-chain plane. To place the carotenoid ZFS principal axes in the molecular frame of the C−P−C_{60} triad, the low-energy average molecular conformations have been considered. A conformational analysis, based on NMR spectroscopic studies and molecular mechanics calculations, was performed on a carotene−porphyrin dyad model system for the carotene−porphyrin portion of triad **1**.[44] The molecular dyad has an extended conformation, with the carotenoid moiety directed away from the porphyrin ring.

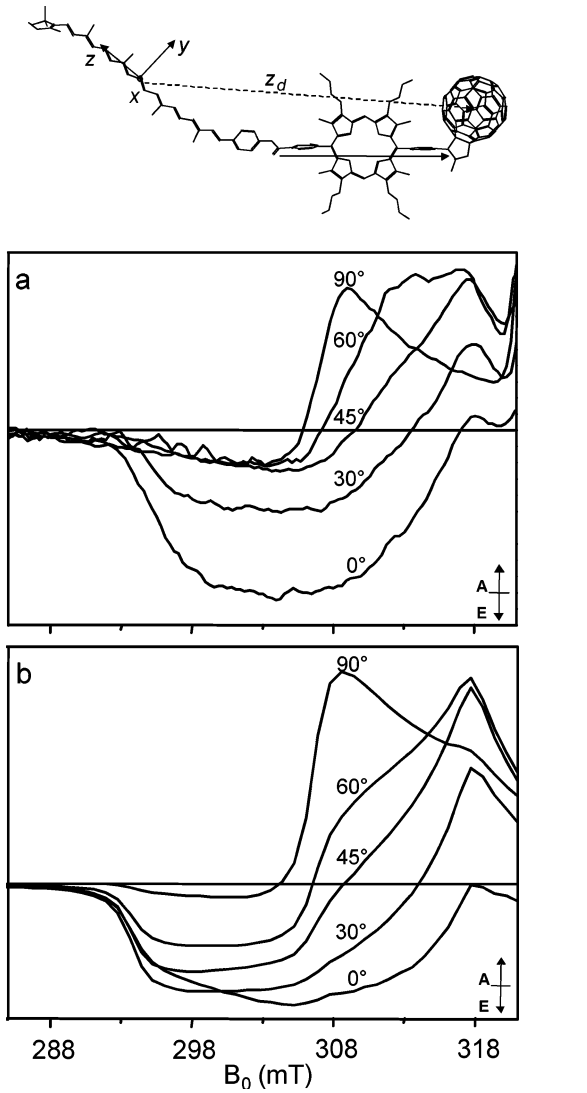

Figure 3. Top: representative energetically favored conformation of triad **1** showing the long axis direction as defined in the text, the principal axes of the ZFS tensor of ^{3}C−P−C_{60}, and the dipolar vector z_d of $C^{\bullet+}$−P−$C_{60}^{\bullet-}$. Bottom: (a) X-band triplet TREPR semispectra of ^{3}C−P−C_{60} at 900 ns after the laser pulse, in the crystalline phase of E-7 ($T = 150$ K) at different angles θ of **L** with respect to **B**. (b) Partially ordered triplet spectra simulations at the same angles θ. The simulation parameters are reported in the text. A = absorption, E = emission.

Molecular modeling of triad **1** confirms the results obtained on the model dyad. In this framework, the carotenoid triplet z axis is located at 30° from the long molecular axis, defined as the molecular axis joining the two phenyl groups, which function as bridges to the carotenoid and fullerene moieties (the long axis in the molecular framework is shown as a solid arrow in the structure given in Figure 3).

To reproduce the experimental orientational dependence in the calculated EPR spectra, the z axis of the ZFS tensor must be located at 40° ± 5° from the molecular alignment axis. Combining the outcome of the analysis with the information on the location of the ZFS axes in the molecular frame, it is possible to asses that the alignment axis is almost parallel to the long axis of the molecule, as defined above, and the orientation of the molecular triad in the LC is therefore dictated by the long molecular axis. The choice of a simple form for the orienting potential finds justification in the result of the

(42) Segre, U.; Pasimeni, L.; Ruzzi, M. *Spectrochim. Acta, Part A* **2000**, *56*, 265−271.
(43) Frick, J.; von Schütz, J. U.; Wolf, H. C.; Kothe, G. *Mol. Cryst. Liq. Cryst.* **1990**, *183*, 269−272.
(44) Gust, D.; Moore, T. A.; Moore, A. L.; Devadoss, C.; Liddell, P. A.; Hermant, R.; Nieman, R. A.; Demanche, L. J.; DeGraziano, J. M.; Gouni, I. *J. Am. Chem. Soc.* **1992**, *114*, 3590−3603.

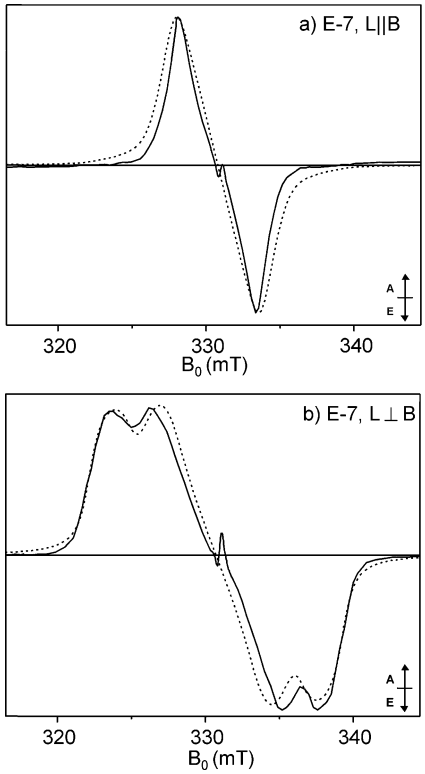

Figure 4. X-band triplet TREPR spectra of C−P−^{3}C$_{60}$ (—) at 250 ns after the laser pulse in the crystalline phase of E-7 (T = 150 K) and the corresponding partially ordered triplet spectra simulations (- - -): (a) at the parallel configuration between the LC director and the external magnetic field (**L** || **B**) and (b) at the perpendicular configuration (**L** ⊥ **B**). The simulation parameters are reported in the text. A = absorption, E = emission.

simulations: the long molecular axis is indeed the symmetry axis of the molecule. The likely presence of several conformers, produced by rotation around the single bonds of the linkage joining the porphyrin and carotenoid moieties[44] does not affect the outcome of the simulations, since they are all included in the cylindrical distribution of the molecules around the ordering director. In previous studies on porphyrin systems partially ordered in LC matrices,[45,46] the orientation distribution has been taken as the product of two Gaussian distribution functions, describing the in-plane orientation of the porphyrin molecule with respect to **L** and the fluctuations of the molecular plane about **L**. Assuming that this or a more general form for the orientational distribution function would be more appropriate for describing the solvent−solute interactions, the spectra corresponding to different conformers should be added together. Summation of the spectra corresponding to the conformers reported in ref 44 reduces the agreement with the experimental orientation dependence of the EPR spectra.

Simulations of the partially ordered spectrum of the fullerene triplet have also been performed. In Figure 4 the TREPR spectra 250 ns after the laser pulse, in the fullerene triplet spectral range, are shown for the parallel and perpendicular configuration of **L** in the crystalline phase of E-7 (T = 150 K). The calculated spectra are superimposed on the experimental spectra of the fullerene triplet state in the partially ordered glass. The features in the central part of the spectra, which belong to the radical pair state, are not simulated. The ZFS parameters ($|D|$ = 0.0080 cm^{-1}, $|E|$ = 0.0007 cm^{-1}) and the relative population rates (A_x = 1.0, A_y = 0.3, A_z = 0.01) of the triplet spin sublevels used in the simulations are those derived for an *N*-methylfulleropyrrolidine molecule whose triplet state is populated by spin−orbit selective ISC from the corresponding singlet state in the LC E-7.[41,47] As in the isotropic solvents,[1,17,21] the fullerene triplet is formed by normal ISC and is only a side product of the photoprocess of molecular triad **1**. No charge separation occurs from the excited singlet state of the fullerene molecule under the conditions of these experiments.

In contrast with the experimental findings on the triplet state of the fullerene molecule and derivatives,[41,48] no dynamic averaging of the ZFS anisotropy has been detected in the overall range of the temperatures corresponding to the crystalline and nematic phases. For fullerene systems, dynamic averaging has been attributed to the interchange among distorted Jahn−Teller configurations.[48,49] In the molecular triad the pseudorotation is not effective, probably due to the functionalization of the fullerene moeity with the carotene−porphyrin portion of the molecule.

The order parameter derived from the simulations of the orientational dependence of the carotenoid triplet spectra has been introduced in the calculations of the fullerene triplet spectra. In the **L** || **B** configuration, the partially ordered triplet spectrum shows contributions from the *xy* principal plane of the ZFS tensor while the *z* principal direction is partially excluded. The rotation by 90° of the sample, which produces the **L** ⊥ **B** configuration, brings the *z* principal direction in the magnetic field direction. An orientation of the *y* principal ZFS axis, corresponding to the intermediate value *Y* of the ZFS tensor in our notation, parallel to the C_2 axis of the *N*-methylfulleropyrrolidine moiety,[41] is compatible with the hypothesis derived from the carotene triplet spectra simulations that the long molecular axis, defined above, dictates the orientation of the molecular triad in the LC. The low-energy average molecular conformations of the C−P−C$_{60}$ triad, derived from molecular modeling, have been considered to place the *y* principal axis of the fullerene triplet ZFS tensor in the overall frame of the molecular system. The different conformers produced by rotation around the single bonds of the linkage joining the porphyrin and the fullerene moieties are all included in the cylindrical distribution around the director, as they are for the carotene−porphyrin portion of the molecule.

In Figure 4, important information concerning the radical pairs, which will be discussed in the next paragraphs, is also present: no phase inversion of the polarization pattern of the radical pair e/a line is produced upon rotation of the sample from the parallel (**L** || **B**) to the perpendicular configuration (**L** ⊥ **B**).

To further investigate the spectral differences between the parallel and perpendicular configurations, the TREPR study was also performed on triad **1** in the ZLI-1167 liquid crystal. The complementary orientation properties of E-7 and ZLI-1167, due to opposite values for $\Delta\chi$,[31] are used to obtain the parallel and

(45) Regev, A.; Levanon, H.; Murai, T.; Sessler, J. L. *J. Chem. Phys.* **1990**, *92*, 4718−4723.
(46) Michaeli, S.; Soffer, S.; Levanon, H.; Senge, M. O.; Kalisch, W. W. *J. Phys. Chem. A* **1999**, *103*, 1950−1957.
(47) Pasimeni, L.; Hirsch, A.; Lamparth, I.; Herzog, A.; Maggini, M.; Prato, M.; Corvaja, C.; Scorrano, G. *J. Am. Chem. Soc.* **1997**, *119*, 12896−12901.
(48) Regev, A.; Gamliel, D.; Meiklyar, V.; Michaeli, S.; Levanon, H. *J. Phys. Chem.* **1993**, *97*, 3671−3679.
(49) Reed, C. A.; Bolskar, R. D. *Chem. Rev.* **2000**, *100*, 1075−1120.

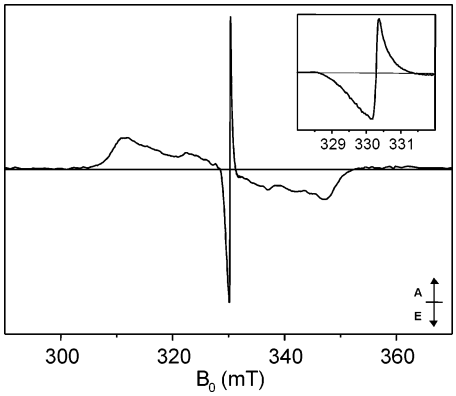

Figure 5. X-band TREPR spectra of the C−P−C_{60} triad in the nematic phase (T = 320 K) of the LC ZLI-1167 (**L** ⊥ **B**), at 350 ns after the laser pulse. The inset displays the expanded TREPR spectra in the radical pair region. A = absorption, E = emission.

perpendicular configurations also in the nematic phase of the LC, where the radical pair signal is the main contribution to the spectrum and the fullerene triplet has lost intensity and therefore does not affect the radical pair line shape. In the fluid nematic phase, rotation of the sample with respect to the magnetic field to produce the perpendicular configuration is not possible, since molecular reorientation brings the molecules back to the initial parallel orientation.

TREPR in the Liquid Crystal ZLI-1167. Figure 5 shows the X-band spin-polarized EPR spectrum at 350 ns after the laser pulse, in the nematic phase of ZLI-1167 at 320 K. The main contribution to the spectrum, as in the nematic phase of E-7, is the narrow $C^{\bullet+}-P-C_{60}^{\bullet-}$ radical pair signal at the center. The partially ordered carotenoid triplet signal shows a similar orientation selection as the one achieved for **L** ⊥ **B** in the crystalline phase of E-7, after sample rotation of 90° (see panel a of Figure 3).

On the other hand, in the nematic phase of ZLI-1167, the fullerene triplet contribution has almost disappeared. This is due to a combination of spin−lattice relaxation effects and the orientation selection, which reduces the contribution of the fullerene signal in the **L** ⊥ **B** configuration. The spin-polarized radical pair, the carotenoid, and fullerene triplet signals have also been detected in the crystalline phase of ZLI-1167 at 150 K and in the smectic phase at 298 K (data not shown). In the isotropic phase at 360 K, as in the case of the LC E-7, only the radical pair and the carotenoid triplet have been detected (data not shown).

Looking in more detail at the spin-polarized radical pair spectrum (see the inset of Figure 5), the same e/a spin polarization pattern is observed for the **L** ⊥ **B** configuration of ZLI-1167 as for the **L** || **B** configuration of E-7 (see insets a of Figure 2). This behavior was already pointed out for the TREPR experiments performed in the crystalline phase of E-7 where the director orientation was varied by sample rotation. Using the ZLI-1167 LC, the perpendicular orientation has been obtained without changing the sample configuration. Furthermore, in the nematic phase of both LCs the radical pair signal is the most important contribution to the spectrum allowing clear-cut comparison between the parallel and perpendicular configurations. The invariance of the phase of the spectrum when going from the parallel to the perpendicular configuration can be discussed in terms of the correlated radical pair sign rule.[50] Inversion of the polarization in one configuration with respect to the other is expected when the dipolar interaction is the main contribution to the splitting of the spectrum. Even if the peak-to-peak separation is not expected to be strongly affected by the orientation of the ZFS principal axes because the inhomogeneous broadening is the dominant feature of the line shape for the $C^{\bullet+}-P-C_{60}^{\bullet-}$ radical pair, phase inversion should still be detectable. For this reason the exchange interaction must contribute substantially to the splitting of the spectrum.

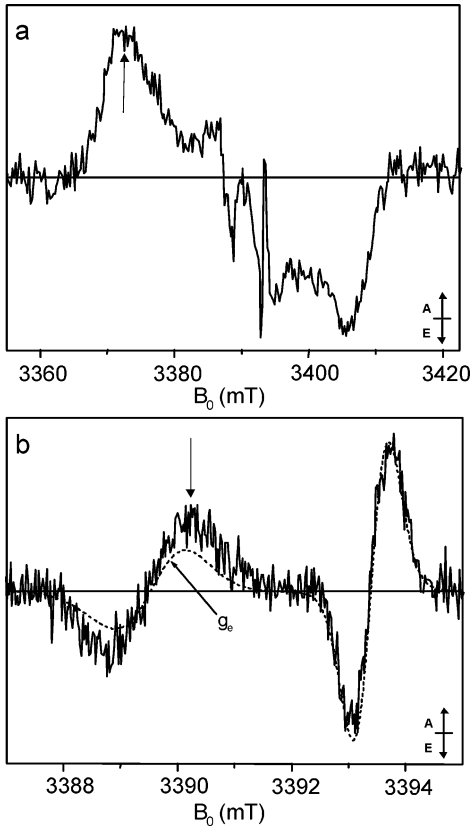

Figure 6. W-band TREPR spectrum of the C−P−C_{60} triad in the nematic phase (T = 320 K) of the LC ZLI-1167 (**L** ⊥ **B**) at 50 ns from the laser pulse with an integration window of 100 ns: (a) carotenoid triplet spectral region, (b) enlargement of the $C^{\bullet+}-P-C_{60}^{\bullet-}$ radical pair spectral region and the corresponding spin-correlated radical pair spectrum simulation (- - -). A linear baseline correction has been applied to the experimental spectrum in inset b.The simulation parameters are reported in Table 1. A = absorption, E = emission.

In the case of the ZLI-1167 LC solvent, the radical pair spectrum shows again only one EPR doublet in antiphase corresponding to the fullerene radical, but is also accompanied by a low-field spectral broadening which is indicative of the presence of the doublet corresponding to the carotenoid radical. This broad feature was obscured in E-7 by the superposition with the fullerene triplet signal. To clarify this point and demonstrate that it is indeed the spectrum of a correlated radical pair, the investigation has been extended to higher fields performing W-band time-resolved EPR experiments on triad **1** embedded in the LCs E-7 and ZLI-1167.

Figure 6 shows the W-band TREPR spectrum in the nematic phase of ZLI-1167 at 320 K. While in the top panel (a) the overall spectrum is presented, the bottom panel (b) is the enlargement of the radical pair region, both taken at 50 ns after

(50) Hore, P. J. In *Advanced EPR*; Hoff, A. J., Ed.; Elsevier Science Publishers B.V.: Amsterdam, 1989; pp 405−440.

the laser pulse at the maximum of the radical pair signal, with an integration window of 100 ns.

The W-band experiment, with the improved spectral resolution, finally shows both spin-polarized derivative-like EPR lines of the radical pair. The same W-band experiment, performed on the triad embedded in the LC E-7, does not show the complete radical pair spectrum due to the still large contribution of the fullerene triplet in the nematic phase of E-7 which, at higher frequencies, obscures completely the carotenoid radical cation doublet and even part of the narrower fullerene radical anion doublet (data not shown).

Simulations performed on the partially ordered W-band spectrum allowed unambiguous identification of the two partners of the charge-separated radical pair, the carotene radical cation and the fullerene radical anion, and derivation of the magnetic interaction parameters between the two spins of the radical pair. The calculated TREPR spectrum of the spin-correlated radical pair has been superimposed to the experimental spectrum in panel b of Figure 6.

The simulations have been performed in the correlated radical pair mechanism framework,[50] which has been extended to partially ordered samples by introducing a Gaussian orientational distribution function. This function has been independently estimated from the analysis of the partially oriented carotenoid triplet spectra, taking into account the complementary configuration of the LC director versus **B** for ZLI-1167. No important variation in the orientation distribution should occur when going from the nematic to the crystalline phase or vice versa. Assuming that the photochemistry of triad **1** in the LC solvent is similar to that in the isotropic solvents, as will be discussed later in the text, the spin correlated radical pair is generated by a singlet precursor and the spin polarization develops in the secondary $C^{\bullet+}-P-C_{60}^{\bullet-}$ radical pair, since the lifetime of the $C-P^{\bullet+}-C_{60}^{\bullet-}$ is likely too short to produce any spin polarization. While the exchange interaction J has been derived from the best-fit simulations, the dipolar interaction, which is described by an axial ZFS tensor, has been estimated in the point-dipole approximation ($D = -0.6$ G), given the large distance between the two radicals (center to center ≈ 36 Å). The distance has been obtained from molecular modeling calculations on triad **1**. The dipolar axis z_d is roughly parallel to the long axis of the molecule (see Figure 3). The radical magnetic parameters, G-tensors and line widths at half-height ($\Delta H_{1/2}$), which simulate the homogeneous broadening and the unresolved inhomogeneous structure, are in good agreement with the corresponding values for the carotene and the *N*-methylfulleropyrrolidine radical model compounds, derived from X-band and high field CW-EPR experiments.[51−56] The same inhomogeneous line width has been assumed for the three components of each radical G-tensor to avoid introducing extra parameters in the simulations. The parameters used in the spectral simulation are summarized in Table 1.

Table 1. Spectral and Kinetic Parameters Used for the $C^{\bullet+}-P-C_{60}^{\bullet-}$ Radical Pair Spectra Simulation Reported in Figure 6b and Figure 8b According to the Model Described in the Result Section (the Parameters Are Discussed in the Text)

SPECTRAL PARAMETERS				
G-tensors [a]	g_{xx}	g_{yy}	g_{zz}	$\langle g \rangle$ [b]
$C^{\bullet+}$	2.00335	2.00251	2.00227	2.00271
$C_{60}^{\bullet-}$	—	—	—	2.00023
Spin-spin coupling of $C^{\bullet+}PC_{60}^{\bullet-}$				
D	-0.6 G			
J	+0.5 ± 0.2 G			
Tensor orientations [c]	α	β	γ	
G-tensor of $C^{\bullet+}$	90°	90°	30°	
D-tensor of $C^{\bullet+}PC_{60}^{\bullet-}$	0°	0°	0°	
$\Delta H_{1/2}$ [d]				
$C^{\bullet+}$	12 G			
$C_{60}^{\bullet-}$	7 G			
DYNAMIC PARAMETERS				
k_T [e]	1.5×10^7 s^{-1}			
k_S [e]	2.5×10^6 s^{-1}			
Q [f]	3.4×10^8 s^{-1}			

[a] Estimated error: ±0.00005. [b] The isotropic *g*-value. [c] The tensor orientation expressed in terms of Euler angles are given for rotation about Z by α, Y′ by β, and Z′ by γ. Estimated error: ±5°. [d] $\Delta H_{1/2}$ is the full line width at half-height. Uncertainty: ±5%. [e] Uncertainty: ±10%. [f] $2Q$ is the singlet−triplet mixing frequency.

To reproduce the experimental separation between the two e/a lines of the radical pair, the principal axis corresponding to the g_{xx} component of the carotene G-tensor, which is directed along the polyene long axis,[52] was rotated by 30° from the Z direction defined by the molecular alignment axis. The g_{yy} component, being parallel to the hydrogen bonds of the polyene chain,[52] was consequently rotated by 60° from the Z direction. Molecular modeling calculations, as already stated above, suggest that the carotene chain axis is located at 30° from the long molecular axis, defined as the axis along the two phenyl bridging groups. The orientation of the G-tensor principal axes is consistent with the carotene triplet spectra simulations identifying the alignment axis with the long molecular axis. The fullerene doublet, on the other hand, is best simulated with an isotropic signal, with a *g*-value below the free electron value, in the range expected for fullerene derivatives.[54,56] The absence of anisotropy in the EPR signal at high temperatures has been attributed to dynamic averaging of different Jahn−Teller distorted forms.[49,56] This phenomenon should find a counterpart in the reduction of the ZFS parameters in the EPR spectrum of the fulleropyrrolidine triplet state, which should occur in a similar temperature regime. No dynamic effect has been detected however either in X-band, as already pointed out, or in W-band in the triplet state signal. Alternatively, the only way to introduce the rhombic G-tensor anisotropy[56] in the radical pair spectrum simulations is to keep the g_{zz} component parallel to the Z direction and, therefore, in the case of ZLI-1167 LC, exclude it completely from the plane spanned by the static magnetic field. The anisotropy contribution in the x and y directions of the G-tensor is small, which is in agreement with the fullerene doublet appearing almost symmetric in the EPR spectrum.

In this way the spin correlated radical pair EPR signal can be definitively assigned to the secondary charge-separated state $C^{\bullet+}-P-C_{60}^{\bullet-}$. The best value for the exchange interaction parameter J, which is the variable parameter in the simulations,

(51) Lakshmi, K. V.; Reifler, M. J.; Brudvig, G. W.; Poluektov, O. G.; Wagner, A. M.; Thurnauer, M. C. *J. Phys. Chem. B* **2000**, *104*, 10445−10448.
(52) Faller, P.; Rutherford, A. W.; Un, S. *J. Phys. Chem. B* **2000**, *104*, 10960−10963.
(53) Grant, J. L.; Kramer, V. J.; Ding, R.; Kispert, L. D. *J. Am. Chem. Soc.* **1988**, *110*, 2151−2157.
(54) Sun, Y.; Drovetskaya, T.; Bolskar, R. D.; Bau, R.; Boyd, P. D. W.; Reed, C. A. *J. Org. Chem.* **1997**, *62*, 3642−3649.
(55) Zoleo, A.; Maniero, A. L.; Prato, M.; Severin, M. G.; Brunel, L. C.; Kordatos, K.; Brustolon, M. *J. Phys. Chem. A* **2000**, *104*, 9853−9863.
(56) Brustolon, M.; Zoleo, A.; Agostini, G.; Maggini, M. *J. Phys. Chem. A* **1998**, *102*, 6331−6339.

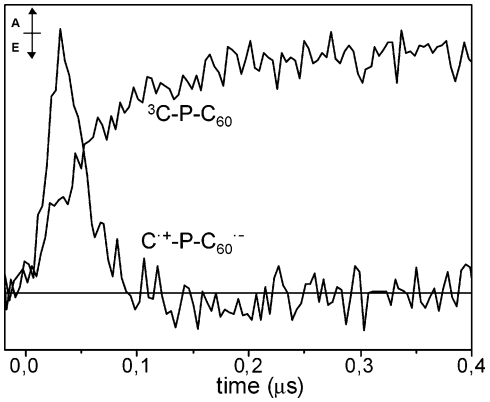

Figure 7. W-band TREPR kinetic traces of the $C^{\bullet+}-P-C_{60}^{\bullet-}$ radical pair and of the carotenoid triplet state in the nematic phase (T = 320 K) of ZLI-1167 (**L** ⊥ **B**). The field positions at which the signals have been recorded are shown with arrows in Figure 6. A = absorption, E = emission.

was obtained by a simultaneous fit of the W-band radical pair spectrum and the X-band spectra in the parallel and perpendicular configurations. The simulations which give the best agreement with the experimental spectra are characterized by a J parameter value of $+0.5 \pm 0.2$ G, confirming that in this and similar carotenoid−porphyrin−fullerene model systems the exchange interaction makes a substantial contribution to the total spin−spin coupling of the $C^{\bullet+}-P-C_{60}^{\bullet-}$ radical pair, despite the large separation between the $C^{\bullet+}$ and the $C_{60}^{\bullet-}$ radicals.[17,21] The positive value of J is a required condition, as already proved[17] to obtain in the calculated spectra the same e/a polarization pattern for each radical pair doublet as in the experimental spectra.

The spectral information on the molecular order obtained from the simulations of the partially ordered spectra is accompanied by dynamic information contained in the time evolution of the TREPR spectra.

The increased time-resolution in the W-band experiment allowed us to follow the time evolution of both the $C^{\bullet+}-P-C_{60}^{\bullet-}$ radical pair and the carotenoid triplet EPR signals at 320 K in the nematic phase of ZLI-1167 (see Figure 7). The field positions at which the kinetic traces have been recorded are shown with arrows in Figure 6a and 6b. The signals have been normalized at their maxima to show the correlation between the radical pair signal decay and the rise of the carotenoid triplet signal. This correlation is further proof that in the LC ZLI-1167 the carotenoid triplet is also formed by charge recombination of the secondary radical pair.

In panel a of Figure 8 the overall radical pair spectrum for the W-band is shown at different delays from the laser pulse, in the nematic phase of ZLI-1167 at 320 K. An asymmetric time evolution of the two lines belonging to each of the radical pair doublet, with the inner lines disappearing faster than the outer lines characterizes the radical pair dynamics. The asymmetry in the time evolution of the EPR spectrum is indicative of a specific dynamic behavior of the $C^{\bullet+}-P-C_{60}^{\bullet-}$ radical pair.

In the framework of the spin-correlated radical pair, in which the kinetics of recombination depend on the singlet−triplet mixing in the radical pair and on the singlet and triplet recombination rate constants,[57,58] different kinetics for the two antiphase components of the individual radical pair doublet are due to a faster recombination to the triplet state than to the singlet ground state or vice versa. If the singlet recombination rate k_S and the triplet recombination rate k_T are different, the radical pair states **2** and **3**, in the notation of P. Hore,[50] having different singlet character, will depopulate at different rates depending on the singlet−triplet mixing term Q, on the magnetic interaction parameters D and J as well as on k_S and k_T. The two contributions of each doublet in antiphase will therefore no longer be of equal intensity during their time evolution.

In panel b of Figure 8 the simulated time development of the TREPR spectrum is compared with the experimental one. The simulations reproduce the faster kinetics of the inner lines compared to the outer lines. In the model used for the simulations, the spin dynamics of the radical pair are described by the stochastic Liouville equation, in which singlet−triplet mixing in the correlated radical pair, singlet and triplet recombination, and spin relaxation are included.[57,59] The same spectral parameters used in the simulation of the initial spin-polarized radical pair spectrum (see Figure 6b), which are summarized in Table 1, were used in the simulation of the time development of the EPR spectrum. The kinetic parameters, which are also reported in Table 1, were chosen to give the best agreement with the experimental behavior.

The experimental behavior of the inner lines of the radical doublets, disappearing more quickly than the outer components, can be reproduced in the simulations only if the triplet recombination rate is faster than the rate of recombination to the singlet ground state. Keeping the parameter k_T fixed to the best-fitting value ($k_T = 1.5 \times 10^7$ s^{-1}), the maximum value for k_S, which is still compatible with the experimental behavior, is 2.5×10^6 s^{-1}. A faster singlet recombination rate would reduce the asymmetry of the EPR doublets and invert the order of asymmetry when it become faster than k_T, while slower k_S values are always in agreement with the experimental time dependence. Thus, the asymmetric time evolution of the radical pair spectrum, which is accompanied by the detection of the carotenoid triplet state characterized by the specific recombination spin polarization pattern, proves that, in the LC ZLI-1167, in the same way as in the isotropic solvents, triplet recombination is the main route of decay for the $C^{\bullet+}-P-C_{60}^{\bullet-}$ radical pair. A further check consists of introducing a triplet recombination rate k_T of 1.5×10^7 s^{-1} in the fit of the kinetic trace of the carotenoid triplet signal reported in Figure 7. The fitting function is composed of an exponential rise, with a time constant ($1/k_T$) relative to the process of triplet recombination of the radical pair, and an exponential decay characterized by a time constant, which is in agreement with the carotenoid triplet lifetime.[1] If triplet decay is the main route and singlet−triplet mixing is fast compared to the radical pair decay process, the same value for k_T should be compatible with both the radical pair signal decay and the recombination triplet formation. This was indeed the case.

The asymmetric behavior in the decay of the EPR components can also be produced combining the triplet decay with a spin lattice relaxation effect. If a spin lattice relaxation rate W_1 of 4×10^6 s^{-1} is introduced as a simulation parameter, k_T slows down to 1.2×10^7 s^{-1}, remaining, however, the main decay route of the spin-correlated radical pair. The spin−lattice

(57) Till, U.; Hore, P. J. *Mol. Phys.* **1997**, *90*, 289−296.
(58) Till, U.; Klenina, I. B.; Proskuryakov, I. I.; Hoff, A. J.; Hore, P. J. *J. Phys. Chem. B* **1997**, *101*, 10939−10948.
(59) Fuhs, M.; Elger, G.; Osintsev, A.; Popov, A.; Kurreck, H.; Möbius, K. *Mol. Phys.* **2000**, *98*, 1025−1040.

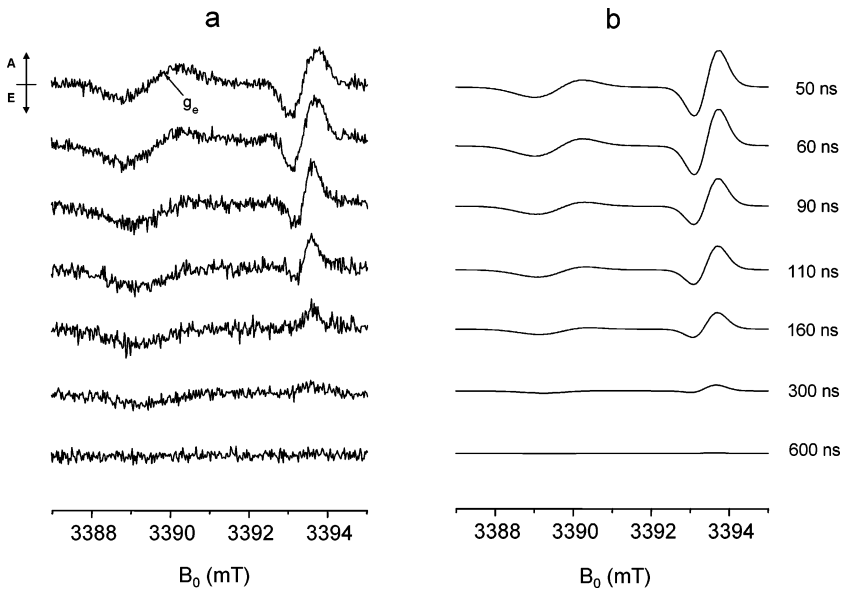

Figure 8. (a) Time-evolution of the W-band TREPR spectrum of the $C^{\bullet+}-P-C_{60}^{\bullet-}$ radical pair in the nematic phase ($T = 320$ K) of ZLI-1167 (**L** $\perp$ **B**). (b) Simulations based on the model described in the result section and the parameters reported in Table 1. The delay times after the laser pulse are listed on the right side, the corresponding integration window is 5 ns. A = absorption, E = emission.

relaxation rate contributes together with k_T to reduce the spin-polarized intensity of the two EPR e/a lines, but it cannot exceed k_T or produce by itself the experimental dynamic behavior, since it would lead to a Boltzmann spin population distribution and not to the faster and selective disappearance of the two inner lines of the spectrum. A further proof that the spin relaxation cannot be the main contribution to the spin dynamics comes from the experiments in the isotropic phase of both LCs: a spin-polarized radical pair signal has been detected also at high temperatures where the isotropic phase of the LC is reached; this signal does not evolve to the Boltzmann population during the radical pair lifetime.

Triplet recombination is the main decay route also in the nematic phase of the LC E-7. In this case, an asymmetric time evolution of the two lines belonging to the only visible radical pair doublet, with the low-field line disappearing faster than the high-field line, and a slight phase inversion of the spin polarization characterize the radical pair dynamics (data not shown). The asymmetric kinetic behavior can be explained again in terms of a faster triplet recombination route compared to the singlet recombination route. The static parameters reported in Table 1 have been used successfully to simulate the time development of the radical pair spectrum in the nematic phase of E-7. The kinetic parameters have been varied to take into account the different temperatures at which the experiment was performed (data not shown).

The polarization phase inversion of both lines belonging to the fullerene doublet was already reported[21] and ascribed to the activation of a triplet-initiated route for the population of the radical pair in the nematic phase of E-7. This route is not active in the crystalline phase, where the TREPR spectrum does not exhibit any phase inversion in time and becomes active only at temperatures in which the nematic phase of the LC solvent is reached. No evidence of a triplet-initiated radical pair was found for triad **1** in the 2-MeTHF glass in the previous TREPR study on the same molecular triad[21] and in the LC ZLI-1167 in the present investigation.

Discussion

A multifrequency time-resolved EPR investigation in X-band and W-band has been performed on triad **1** embedded in the two liquid crystals E-7 and ZLI-1167, which are characterized by complementary orientation properties. The multifrequency approach together with the employment of liquid crystals for the study of the photoinduced ET in the $C-P-C_{60}$ molecular triad has been very important in elucidating different aspects of the ET process that will be discussed in detail in the next paragraphs.

The W-band TREPR radical pair spectrum shows both antiphase doublets, confirming the spin-correlated nature of the radical pair and allowing final identification of the two partners of the charge-separated state: the carotene radical cation and the fullerene radical anion.

The molecular triad undergoes two-step photoinduced charge separation in the different phases of the ordered media. The secondary spin-polarized radical pairs $C^{\bullet+}-P-C_{60}^{\bullet-}$ and the recombination triplet $^3C-P-C_{60}$ have been detected by TR-EPR. Simulations have allowed unambiguous identification of the paramagnetic species. The fullerene triplet signal has also been detected. Direct excitation of the fullerene moiety yields the singlet excited state that decays by normal ISC to give the fullerene triplet state.

Even in the crystalline phase, where the motions of the solvent molecules are restricted, charge separation is still active. High yield charge separation in the isotropic glass phase down to cryogenic temperatures was already demonstrated.[1,21] Photo-induced ET in most model reaction centers ceases at low temperature when the solvent becomes glassy. Few exceptions are reported.[28,29] The ability of the $C-P-C_{60}$ triad to mimic low-temperature charge separation derives more from the specific molecular properties of the fullerene molecule than from the dielectric properties of the anisotropic solvent. It has been ascribed to the lack of sensitivity of the fullerene anion to solvent properties due to the spread of charge over many carbon atoms in this large spherical ion.[1] For this reason destabilization of

the initial charge-separated states, upon conversion of the LC solvent to the crystalline phase, is not large enough to render ET thermodynamically impossible. In the nematic fluid phase of the LC, where the charge-separated states are stabilized via solvent dipole relaxation, the yield of two-step charge separation is increased as demonstrated by the fact that the radical pair signal becomes the major contribution to the TREPR spectrum.

We have also shown that another important property of molecular triad **1** is demonstrated in the LC medium: charge recombination to the triplet state in high quantum yields. Triplet recombination occurs in all the different phases of the LC. The partially ordered carotenoid triplet spectrum is characterized by a spin polarization pattern deriving from the triplet recombination mechanism, as proven by simulation of the orientation dependence of the spectrum. The high quantum yield of this decay route is demonstrated by the time-evolution of the radical pair spectrum: the asymmetric decay of the two antiphase lines of each of spin-polarized doublet can be ascribed to a faster triplet than singlet recombination rate. The values for the spin-selective recombination rates, derived from the simulation of the time development of the radical pair spectrum and summarized in Table 1, can be used to estimate the triplet yield. Using eq 3[57]

$$\Phi_T = k_T \int_0^\infty \rho_{TT}(t)\, dt = \frac{4k_T Q^2 (k_S + k_T)}{(4Q^2 + k_S k_T)(k_S + k_T)^2 + 16 j^2 k_S k_T} \quad (3)$$

where $j = J + {}^1/_2 D(\cos^2 \xi - {}^1/_3)$ and $2Q$ is the singlet−triplet mixing frequency,[50] a triplet yield of 0.86 was estimated. A slower singlet recombination rate would still give good agreement with the experimental behavior and would correspond to a triplet yield of 1.0. It can be then concluded that recombination to the triplet state is the main route of decay for molecular triad **1** not only in the isotropic solvents[1] but also in the LC medium. The small reorganization energy of **1** contributes to this phenomenon. Charge recombination to the carotenoid triplet has a small thermodynamic driving force and occurs in the normal region of the Marcus parabola.[1] Therefore a lower reorganization energy leads to more rapid triplet charge recombination. At the same time, charge recombination to the singlet ground state, occurring in the inverted region, becomes slower upon reduction of the reorganization energy and it is not competitive with the triplet route. In addition, recombination of $C^{\bullet+}-P-C_{60}^{\bullet-}$ to yield the carotenoid triplet is possible because the triplet state is significantly lower in energy than the charge-separated state.[22]

Important spectral information has been derived from the orientational effects produced by the nematic potential of the LC on the triplet and radical pair spectra. Simulations of the partially ordered EPR spectra of the carotenoid and fullerene triplet states, at different orientations of the director versus the external magnetic field, have proved the high degree of order of the molecular triad in the LC medium and have allowed determination of the orientation of the guest molecules with respect to the alignment axis. The orientation distribution function provided by the triplet spectra has been used in the simulations of the spin-correlated radical pair spectra. Simultaneous fits of the X-band radical pair spectra in the parallel and perpendicular orientation and of the W-band spectrum in the perpendicular configuration were achieved with the magnetic parameters reported in Table 1.

Additional spectral information on the magnetic interaction parameters can be obtained by comparing the parallel (**L** || **B**) and perpendicular (**L** ⊥ **B**) configurations, employing two LC characterized by opposite $\Delta\chi$ properties. The absence of any spectral effect on the radical pair spectra when going from one configuration to the other has been used to restrict the range of reasonable values for the exchange parameter. The exchange integral not only must be different from zero but also must contribute substantially together with the dipolar interaction parameter to the splitting of the radical pair lines,[50] as obtained from spectral simulations. The *D* parameter cannot exceed the *J* parameter by more than a factor of 3. This information has been used to restrict the range of plausible values for the *D* and *J* parameters. In the radical pair spectral simulation, the dipolar interaction is a fixed parameter and has been calculated in the point-dipole approximation. This approximation may be not valid for this molecular system because it neglects the spatial extension of the electronic wave function, which could be quite large for both the carotene and fullerene moieties. If this were the case, restricting the relative values of *J* and *D* parameters would be very important to still be able to discuss the magnetic interaction parameters in terms of the electronic structure of the radical pair. For this reason the ZFS parameter *D* has been calculated also for the minimum (25 Å) and maximum distances (52 Å) between the carotenoid polyene and the fulleropyrrolidine molecule. A $D_{MAX} = -1.7$ G is not compatible with the experimental observations. To avoid phase inversion from the parallel to the perpendicular configuration, the exchange parameter, corresponding to $D = -1.7$ G, should exceed 0.6 G, but the combination of the dipolar and exchange interaction parameters produces too large a splitting of the EPR doublets which is not compatible with the experimental spectra. On the other hand, a $D_{MIN} = -0.2$ G, corresponding to the largest distance, is accompanied in the spin-correlated radical pair simulations by an exchange parameter of 0.8 G, which exceeds the dipolar interaction. These results for the limiting cases allow us to state that the exchange interaction is of the same order of magnitude as the dipolar interaction in the $C-P-C_{60}$ triad.

From the radical pair spectral analysis it can be therefore concluded that the exchange interaction *J* makes an important contribution to the total magnetic spin−spin interaction and is of the same order of magnitude of the evaluated dipole−dipole interaction in the $C^{\bullet+}-P-C_{60}^{\bullet-}$ radical pair. An exponential dependence of the exchange interaction on the spin−spin separation[60] would make the exchange integral negligible compared to the dipolar interaction, based on the spatial separation of the two radicals in the molecular triad. All this information confirms the hypothesis, already stated in previous papers on the $C-P-C_{60}$ triads,[17,21] of an electronic interaction between the donor and acceptor moieties in the radical pair mediated by the porphyrin bridge.

The exchange interaction parameter in the $C^{\bullet+}-P-C_{60}^{\bullet-}$ charge transfer state, derived from spectral simulations, has been used for evaluating the electronic coupling matrix element *V* of the ET reaction between this state and the electronic states that are energetically close. The singlet−triplet splitting within the radical pair ($2J$) is a sum of the squares of the electronic coupling elements with the ground state and the nearby excited

(60) Herring, C.; Flicker, M. *Phys. Rev.* **1964**, *134*, A362−A366.

states, weighted by the energy splitting between the radical pair state and these states:[33,34,36]

$$2J = E_S - E_T = \left[\sum_n \frac{V_n^2}{\Delta E_n}\right]_S - \left[\sum_n \frac{V_n^2}{\Delta E_n}\right]_T \quad (4)$$

where ΔE_n is the vertical energy separation between the radical pair state and the interacting state at the equilibrium nuclear configuration of $C^{\bullet+}-P-C_{60}^{\bullet-}$ and can be calculated by adding the free energy difference $\Delta G°$ for the reaction and the total reorganization energy λ ($\Delta E_n = \Delta G° + \lambda$). The individual terms, in both the singlet and triplet manifolds in eq 4, may be ferromagnetic or antiferromagnetic depending on the sign of the energy term. On the basis of the energy splitting term at the denominator,[1] the dominant contribution, in the weighted sum of eq 4, should be the electronic coupling of the $C^{\bullet+}-P-C_{60}^{\bullet-}$ triplet radical pair state with the recombination triplet state $^{T}C-P-C_{60}$. Assuming a similar value for the electronic coupling matrix elements for all the states involved, the contributions from the singlet and triplet states localized on the porphyrin and fullerene moiety can be neglected because of the relatively large energy gaps between the radical pair state and these states (see energy diagram in Figure 1). The interaction with the precursor $C-P^{\bullet+}-C_{60}^{\bullet-}$ radical pair state is not considered, since the singlet and triplet contributions are essentially equal, being characterized by the same electronic coupling matrix elements and energy splitting terms, and therefore they cancel out in eq 4.[61]

A single-term expression for J is therefore obtained:

$$2J = -\frac{V_{CRT}^2}{\Delta E_{CRT}} = -\frac{V_{CRT}^2}{\Delta G°_{CRT} + \lambda} \quad (5)$$

where the energy splitting terms were estimated using the electrochemical data for the free energy $\Delta G° = -0.4$ eV[1] and a value for the reorganization energy $\lambda = 0.5$ eV, which is compatible with the low reorganization energy reported for fullerene-based systems[9,14,62] and with a triplet recombination process lying in the Marcus normal region.[1]

The estimation that the dominant electronic coupling term, which determines the singlet−triplet energy splitting within the $C^{\bullet+}-P-C_{60}^{\bullet-}$ radical pair state is the one that connects this state with the recombination triplet state, is in agreement with the positive value found from simulations for the exchange interaction parameter, corresponding to a ferromagnetic coupling in which the triplet $C^{\bullet+}-P-C_{60}^{\bullet-}$ radical pair state is lower in energy than the corresponding singlet radical pair state. A positive contribution comes from this term, since the energy splitting term at the denominator in eq 5 is negative for the triplet recombination process.

The hypothesis of the involvement of the porphyrin moiety in the exchange interaction between the electron donor and acceptor can be then verified by evaluating the matrix element relative to triplet charge recombination, V_{CTR}, from the exchange interaction parameter J, determined experimentally from the radical pair TREPR spectra. The value obtained for V_{CTR} using eq 5 is 0.27 cm^{-1}. The evaluation of the nonadiabatic electron-transfer rate k_{ET} for triplet charge recombination, using $V_{CTR} = 0.27$ cm^{-1}, $\Delta G° = -0.4$ eV, and $\lambda = 0.5$ eV in the expression derived from the Marcus theory in the high-temperature limit:[63]

$$k_{ET} = \frac{2\pi}{\hbar} V^2 \frac{1}{\sqrt{4\pi\lambda k_B T}} \exp\left[-\frac{(\Delta G° + \lambda)^2}{4\lambda k_B T}\right] \quad (6)$$

results in $k_T = 22 \times 10^6$ s^{-1}, at 292 K. In view of the crude approximations adopted for the calculation, the measured rate constant $k_T = 2.9 \times 10^6$ s^{-1} in 2-MeTHF at 292 K[1] is in acceptable agreement with the estimated value.

In the simplest model, the distance dependence of the electronic coupling matrix element V of ET is exponential. The distance decay constant β has been estimated for different classes of systems, including covalently linked donor−acceptor complexes.[64−66] Estimation of the electronic coupling element at the edge-to-edge distance of 25 Å between the carotene and fullerene moieties, taking from the literature the value of $\beta = 0.9$ $Å^{-1}$ found for donor−acceptor pairs separated by saturated bridging groups,[64] is consistent with the value found for V in the present report. Large values of β (3−5 $Å^{-1}$), expected if the donor and acceptor are separated by the vacuum,[67] would reduce the coupling to zero at such a large edge-to-edge distance. Even assuming a through-solvent mechanism, which for tunneling through aqueous and organic glasses is characterized by a distance factor around 1.2 $Å^{-1}$,[68] the electronic coupling element would be reduced by at least an order of magnitude.

The spectral analysis of the spin-correlated radical pair has allowed determination of not only the static magnetic interaction parameters but also dynamic information on the spin-selective recombination. The value for $k_T = 1.5 \times 10^7$ s^{-1} obtained from the W-band experiments in the nematic phase of ZLI-1167 at 320 K can be compared with the corresponding value obtained in the isotropic 2-MeTHF solvent.[1] For the isotropic solvent, k_T was not measured at this temperature but it was possible to extrapolate the corresponding value from its reported temperature dependence.[1] The extrapolated value for k_T is 5.8×10^6 s^{-1} at 320 K for the isotropic solvent. The comparison between k_T in the isotropic and oriented media suggests that the triplet recombination rate is surprisingly fast in the nematic phase of the LC, even faster than the corresponding rate in the isotropic solvent. The dynamic behavior, as already discussed in the result section, cannot be produced by fast spin−lattice relaxation and can only be ascribed to a fast triplet recombination route. Therefore, dynamic simulations prove that no attenuation effect due to the nematic potential has been produced in the nematic phase of the LC where, as already reported,[37,69,70] the ET reaction dynamics should be brought into the solvent-controlled adiabatic limit. In the adiabatic limit, the ET rate constant is

(61) Marcus, R. A. *Chem. Phys. Lett.* **1987**, *133*, 471−477.
(62) Imahori, H.; Tkachenko, N. V.; Vehmanen, V.; Tamaki, K.; Lemmetyinen, H.; Sakata, Y.; Fukuzumi, S. *J. Phys. Chem. A* **2001**, *105*, 1750−1756.
(63) Marcus, R. A.; Sutin, N. *Biochim. Biophys. Acta* **1985**, *811*, 265−322.
(64) Closs, G. L.; Miller, J. R. *Science* **1988**, *240*, 440−447.
(65) Newton, M. D. *Chem. Rev.* **1991**, *91*, 767−792.
(66) Moser, C. C.; Keske, J. M.; Warncke, K.; Farid, R. S.; Dutton, P. L. *Nature* **1992**, *355*, 796−802.
(67) Beratan, D. N.; Betts, J. N.; Onuchic, J. N. *Science* **1991**, *252*, 1285−1288.
(68) Ponce, A.; Gray, H. B.; Winkler, J. R. *J. Am. Chem. Soc.* **2000**, *122*, 8187−8191.
(69) Hasharoni, K.; Levanon, H.; Gätschmann, J.; Schubert, H.; Kurreck, H.; Möbius, K. *J. Phys. Chem.* **1995**, *99*, 7514−7521.
(70) Shaakov, S.; Galili, T.; Stavitski, E.; Levanon, H.; Lukas, A.; Wasielewski, M. R. *J. Am. Chem. Soc.* **2003**, *125*, 6563−6572.

inversely proportional to the solvent longitudinal dielectric relaxation time τ_L:[71,72]

$$k_{ET}^{ad} = \frac{1}{\tau_L}\sqrt{\frac{\lambda}{16\pi k_B T}}\exp\left[-\frac{(\Delta G^\circ + \lambda)^2}{4\lambda k_B T}\right] \quad (7)$$

The transition from the nonadiabatic (eq 5) to the solvent-controlled adiabatic limit (eq 7) is expressed in terms of the adiabaticity parameter given by:

$$\kappa = \frac{4\pi {V_{DA}}^2 \tau_L}{\hbar\lambda} \quad (8)$$

For $\kappa \ll 1$ the ET kinetics are in the nonadiabatic limit while for $\kappa \gg 1$ the solvent-controlled adiabatic limit is reached.

The experimental observation that the triplet recombination process remains in the nonadiabatic limit in the nematic phase of the LC can be verified by evaluating the V_{CTR} electronic coupling term from eq 8. An adiabaticity parameter of 0.1, which safely brings k_{ET} into the nonadiabatic limit, corresponds to $V_{CRT} = 0.13$ cm^{-1}, using in the calculation an estimated[30] $\tau_L = 10^{-8}$ and $\lambda = 0.5$ eV, which is close to the value estimated from eq 5 ($V_{CRT} = 0.27$ cm^{-1}) using the experimental value of the exchange interaction parameter J. The LC medium is therefore not able to influence the ET kinetics of a weakly coupled donor−acceptor system such as triad **1** for which the ET rate remains proportional to the small electronic coupling term V^2. The dynamic information provides, therefore, further evidence of the validity of the range of values found for the electronic coupling matrix elements of the $C^{\bullet+}-P-C_{60}^{\bullet-}$ radical pair state.

Conclusions

In this multifrequency time-resolved EPR investigation we have demonstrated that the $C-P-C_{60}$ molecular triad features desirable characteristics that make it a good model for artificial photosynthetic reaction centers.

The $C-P-C_{60}$ triad has been successfully embedded in the LC medium, its photochemistry conserving all the important features observed in the isotropic solvents: two-step charge separation in all the different phases of the LC, low-temperature ET behavior, and formation of a triplet state by charge recombination in high yield.

The relative insensitivity of the electron-transfer reactions to temperature even in the liquid crystal medium suggests that the fullerene-based molecular systems may be useful for possible solar energy conversion or optoelectronic applications where photoinduced ET in rigid ordered media is required.

Evaluation of the exchange interaction parameter for the radical pair $C^{\bullet+}-P-C_{60}^{\bullet-}$ has been used to estimate the electronic coupling V of the electron transfer reaction, providing information on the electronic structure of the radical pair. We have demonstrated that the experimentally determined exchange interaction parameter can be related to one specific dominant electronic coupling matrix element. This will allow comparison of the electronic structure of the radical pair in terms of the electronic path connecting the two interacting spins in the whole series of carotene−porphyrin−fullerene molecular triads, in which small structural variations of the porphyrin bridge connecting the donor and acceptor moieties have been produced[1,16,18−20] and relate it to the efficiency of the recombination ET pathway. A detailed study is in progress to determine the effect induced in the electronic coupling by the structural variations. This detailed information is very useful in the design of model system, featuring optimized electron-transfer properties.

Acknowledgment. This work was supported by the PRIN Project No. 2002031443, by the Project Giovani Ricercatori 2001 No. 128 of the University of Padova, by the U.S. NSF Grant No. CHE-0078835 and by the TMR Network of the European Union FMRX-CT98-0214. The authors thank Prof. Klaus Möbius for collaborating on the W-band measurements, Prof. Ulderico Segre for providing the simulation program for partially ordered triplet spectra, and Prof. Alberta Ferrarini for stimulating discussions.

JA046067U

(71) Rips, I.; Jortner, J. *Chem. Phys. Lett.* **1987**, *133*, 411−414.
(72) Rips, I.; Jortner, J. *J. Chem. Phys.* **1987**, *87*, 2090−2104.